


Article

Nano hydroxyapatite-blasted titanium surface affects pre-osteoblast morphology by modulating critical intracellular pathways[†]

Fábio BEZERRA¹, Marcel R. FERREIRA¹, Giselle N. Fontes², Célio Jr da Costa FERNANDES¹; Denise C. Andia³, Nilson C. Cruz⁴, Rodrigo A. da SILVA¹; Willian F. ZAMBUZZI^{1,‡} 

¹Dept. of Chemistry and Biochemistry, Bioscience Institute, State University of São Paulo – UNESP, *campus* Botucatu, Botucatu, São Paulo, Brazil;

²Laboratory of Microscopy Applied to Life Science - LAMAV, Directory of Metrology Applied to Life Science - Dimav, National Institute of Metrology Quality and Technology - INMETRO, Duque de Caxias, RJ, Brazil

³Faculdade de Odontologia – Área de Pesquisa em Epigenética, Universidade Paulista, UNIP, São Paulo/SP, Brasil.

⁴Laboratório de Plasmas Tecnológicos; Instituto de Ciência e Tecnologia, Universidade Estadual Paulista, Sorocaba - SP; 18087-180,

[‡]Corresponding author:

Willian F. Zambuzzi, PhD

Head of Bioassays and Cellular Dynamic Lab,

Dept. of Chemistry and Biochemistry

Biosciences Institute / IBB-UNESP

P.O. Box: 510, Zip Code: 18618-970

Rubião Jr – Botucatu – São Paulo – Brazil

e-mail: wzambuzzi@ibb.unesp.br

Phone: +55 14 3880-0599

[†]This article has been accepted for publication and undergone full peer review but has not been through the copyediting, typesetting, pagination and proofreading process, which may lead to differences between this version and the Version of Record. Please cite this article as doi: [10.1002/bit.26310]

This article is protected by copyright. All rights reserved

Received October 25, 2016; Revision Received March 16, 2017; Accepted April 3, 2017

ABSTRACT

Since intracellular signalling pathways are proposed to predict the quality of cell-surface relationship, this study addressed pre-osteoblast behaviour in response to nano hydroxyapatite (HA)-blasted titanium (Ti) surface by exploring critical intracellular pathways and pre-osteoblast morphological change. Physicochemical properties were evaluated by atomic force microscopy and wettability considering water contact angle of three differently texturized Ti surfaces: Machined (Mac), Dual acid-etching (DAE) and nano hydroxyapatite-blasted (nHA). The results revealed critical differences in surface topography, impacting the water contact angle and later the osteoblast performance. In order to evaluate the effect of those topographical characteristics on biological responses, we have seeded pre-osteoblast cells on the Ti discs for up to 4 hours and subjected the cultures to biological analysis. Firstly, we have observed pre-osteoblasts morphological changes resulting from the interaction with the Ti texturized surfaces whereas the cells cultured on nHA presented a more advanced spreading process when compared with the cells cultured on the other surfaces. These results argued us for analysing the molecular machinery and thus, we have shown that nHA promoted a lower Bax/Bcl2 ratio, suggesting an interesting anti-apoptotic effect, maybe explained by the fact that HA is a natural element present in bone composition. Thereafter, we investigated the potential effect of those surfaces on promoting pre-osteoblast adhesion and survival signalling by performing crystal violet and immunoblotting approaches, respectively. Our results showed that nHA promoted a higher pre-osteoblast adhesion supported by up-modulating FAK and Src activations, both signalling transducers involved during eukaryotic cell adhesion. Also, we have shown Ras-Erk stimulation by the all evaluated surfaces. Finally, we showed that all Ti-texturing surfaces were able to promote osteoblast differentiation up to 10 days, when alkaline phosphatase (ALP) activity and osteogenic transcription factors were up-modulated. Altogether, our results showed for the first time that nano hydroxyapatite-blasted titanium surface promotes crucial intracellular signalling network responsible for cell adapting on the Ti-surface. This article is protected by copyright. All rights reserved

Key words: Biotechnology; Nanotechnology; Hydroxyapatite; Implants; Osteoblast; Adhesion; Signal Transduction.

INTRODUCTION

Over the last decades endosseous implants have been widely used for restoring edentulism (Sohrabi et al., 2012), impacting patients' quality of life. Although research on dental implant designs, materials and techniques has increased in the past few years and is expected to expand in the future, there is still a lot of work involved in the use of better biomaterials, implant design, surface modification and functionalization of surfaces to improve the long-term outcomes of the treatment (reviewed in Gaviria et al., 2014). In order to increase the success rate of dental implants, research has been focused on the control of surface properties such as topography and roughness. Specifically, micro-level features are included to impart osseointegration or direct bone to implant contact at the micro level (Di Liddo et al., 2014; Salou et al., 2015). Nanotopography has been suggested decisive for early osseointegration (Zambuzzi et al., 2014), which enhance new bone formation in vivo (Barkarmo et al., 2014b). In addition, it is known that nanotextured surfaces not only enhance bone formation but also strengthen biomechanical properties (Jimbo et al., 2012).

Surrounding biological response to implanted material is mediated by the interaction of the implant through its surface and in order to further improve the treatment success, modifications on implants surfaces have been extensively proposed since it is the first component to interact with the host (Gemini-Piperni et al., 2014a; Gemini-Piperni et al., 2014b; Henkel et al., 2013). The first step in this response to implants involves the adsorption of specific proteins, lipids, sugar, and ions, establishing an organic coating responsible to guide surrounding cell performance leading to activation of specific genes. Although nanoscaled structures are enhancing factors for osseointegration, the detailed interfacial interactions with osteogenic cells have not been fully addressed. In order to understand such interactions, we have explored cell signalling investigation (Bertazzo et al., 2010a; Bertazzo et al., 2010b; Fernandes et al., 2014; Gemini-Piperni et al., 2014a; Zambuzzi et al., 2011a; Zambuzzi et al., 2011b; Zambuzzi et al., 2012).

In this work, we focused on investigating the molecular mechanism governing osteoblast adhesion on different biotechnologically modified surfaces in order to establish a map of signalling proteins able to guide the development of novel biomedical materials, such as Erk MAPK signalling and FAK/Src involvement. Erk MAPK signalling plays critical roles in skeletal development (Hu et al., 2015; Jiang et al., 2015). Ras/Raf/Mek/Erk axis signaling is activated by various stimuli in eukaryotic cells, transduces extracellular signals into cells and coordinates cellular responses (Asati et al., 2016). In addition, Focal Adhesion Kinase (FAK) and Src activations are involved in the cell signalling upon the integrin activation and have been suggested as biomarkers of cell-biomaterial interface (Bergeron et al., 2016; Cavagis et al., 2014; Zambuzzi et al., 2014).

Since intracellular signalling pathways are able to predict the quality of cell interaction, this study aimed to evaluate the pre-osteoblast behaviour on nano hydroxyapatite-blasted titanium surface by exploring critical intracellular signal pathways. Briefly, our results showed for the first time that nano hydroxyapatite-blasted titanium surface promotes a better nano-environment for cell adapting by up-regulating crucial intracellular signalling network.

MATERIAL AND METHODS

Materials

Three different titanium surfaces (discs) were evaluated in this study: Machined (Mac; control), Dual Acid-Etched (DEA), and acid-etched nanoHA-blasted (nHA). All materials were sterilized by exposure to Gamma irradiation and donated by S.I.N. – Sistema Nacional de Implantes (São Paulo, SP, Brazil). HA nanocrystalline synthesis and titanium modification: samples were surface modified with hydroxyapatite (HA) using the Promimic HAnano-method, a detailed description can be found elsewhere (Gottlander et al., 1997; Meirelles et al., 2008). Briefly, the samples were dipped into a stable particle suspension containing 10 nm in diameter HA particles followed by a heat treatment at 550 °C for 5 min in nitrogen atmosphere. The surfactant-mediated process allows better control of the chemical composition of the coating (Meirelles et al., 2008). Antibodies: Phospho-MEK1/2 (Ser221) (166F8) Rabbit mAb #2338; Phospho-p44/42 MAPK (Erk1/2) (Thr202/Tyr204) Antibody #9101; Phospho-FAK (Tyr397) (D20B1) Rabbit mAb #8556; Phospho-Src Family (Tyr416) (D49G4) Rabbit mAb #6943; Bax (D3R2M) Rabbit mAb (Rodent Preferred) #14796; BCL2L10 Antibody #3869; β -Actin (8H10D10) Mouse mAb #3700 were purchased from Cell Signaling Technology, Inc. (MA, USA).

Surface's characterization of the materials

Atomic force microscopy (AFM)

AFM analyses were performed in order to probe Ti-modified surfaces. In this technique, the AFM tip acts as a “nano profilometer”, being able to generate information on the micro and nano dimensional aspects of the surface (x, y and z axis). Images were acquired via the equipment Bioscope Catalyst (Bruker Corp), and AFM cantilevers also from Bruker (“RTESPA”, $k = 20$ to 80 N/m) were used. The equipment worked under intermittent contact mode and images were taken from 3 different samples (Machined, Double-Acid Etching and nano Hydroxyapatite) and 3 different regions on each sample (border, middle and opposite border). Scans of $3.3 \times 3.3 \mu\text{m}^2$ were taken to check homogeneity.


Water contact angle

An automated goniometer (Ramé Hart, 100-00) has been used to evaluate water wettability and free surface energy through contact angle measurements. Deionized water and diiodomethane have been used as probe liquids and the presented results correspond to the average of 10 measurements.

Cell culture and cytotoxicity assay

MC3T3-E1 (subclone 4), mouse pre-osteoblastic cells, was used in this study. Cells were cultured in alfa-MEM supplemented with 10% of fetal bovine serum (FBS) at 37°C and 5% CO₂. Sub-confluent passages were trypsinized and used in all experiments. For cell viability assay, sterile titanium discs with different texturized surfaces were transferred to Petri dishes containing culture media (α -MEM). After 24 h incubation at 37°C, conditioned medium was collected and tested for cell viability profile. 50x10⁴ cells/mL was seeded in 96-well dish plates and after 24 hours at sub-confluent stage they were incubated for 24 h with those conditioned medium (n=6). An internal control was assayed by keeping the cells exposed solely to conventional culture medium (control). After 24 h, cell viability was evaluated by using MTT assay (Mossman, 1983), a colorimetric method (Synergy II; BioTek Instruments, USA). The concentration of Formazan directly indicated the viability of cells.

Cell adhesion assay

Pre-osteoblast cells were treated with conditioned medium for 24 hours. Thereafter, the cells were trypsinized, counted and then re-seeded at 5x10⁴ cells/mL in 24-well culture plates for 4 h. Briefly, adherent cells were rinsed in warm PBS and fixed in absolute ethanol-glacial acetic acid (3:1; v/v) for 10 min at room temperature and air-dried. The adherent cells were stained with 0.1% crystal violet (w/v) for 10 min at room temperature. Excess dye was removed by decantation and washed twice with distilled water. The dye was extracted with 10% acetic acid (v/v), and the optical density measured at 550 nm using a microplate reader (Biotek Co., Winooski, VT). Data from each experiment were analysed with six observations in each group. 

Scanning Electron Microscopy (SEM)

Pre-osteoblasts were seeded on different titanium surfaces at the density of 5x10⁴ cells/disc. After 4 h, cells were fixed with 2.5% of glutaraldehyde in 0.1 M phosphate buffer pH 7.3 for 24 h. They were immersed in osmium tetroxide 0.5% for 40 minutes, dehydrated through a series of alcohols, dried at critical point, and finally metallized. Samples were studied using a Quanta 200 - FEI Company scanning electron microscope at an accelerating voltage of 12.5

kV. EDX analyses were performed with 20 kV to evaluate the x-ray characteristics of Ca and Ti in the samples.

Immunoblotting

Cells were directly cultured on different texturized titanium surfaces and after 4 hours they were lysated [Lysis Cocktail (50 mM Tris [tris(hydroxymethyl)aminomethane]–HCl [pH 7.4], 1% Tween 20, 0.25% sodium deoxycholate, 150 mM NaCl, 1 mM EGTA (ethylene glycol tetraacetic acid), 1 mM *O*-Vanadate, 1 mM NaF, and protease inhibitors [1 µg/mL aprotinin, 10 µg/mL leupeptin, and 1 mM 4-(2-amino-ethyl)-benzolsulfonyl-fluorid-hydrochloride])] for 2 h on ice in order to obtain protein extracts. After clearing by centrifugation, the protein concentration was determined using Lowry method. An equal volume of 2x sodium dodecyl sulfate (SDS) gel loading buffer (100 mM Tris-HCl [pH 6.8], 200mM dithiothreitol [DTT], 4% SDS, 0.1% bromophenol blue, and 20% glycerol) was added to samples and boiled for 5 minutes. Proteins extracts were resolved by SDS-PAGE (10 or 12%) and transferred to PVDF membranes (Bio-Rad, Hercules, CA, USA). Membranes were blocked with either 1% fat-free dried milk or bovine serum albumin (2.5%) in Tris-buffered saline (TBS)–Tween 20 (0.05%) and incubated overnight at 4° C with appropriate primary antibody at 1:1000 dilutions. After washing in TBS-Tween 20 (0.05%), membranes were incubated with horseradish peroxidase-conjugated anti-rabbit, anti-goat or anti-mouse IgGs antibodies, at 1:2000 dilutions, in blocking buffer for 1 hour. Thereafter, for detecting the bands we have used enhance chemiluminescence (ECL).

Quantitative PCR assay (qPCR)

Total RNA was extracted from cells with Ambion TRIzol Reagent (Life Sciences - Fisher Scientific Inc, Waltham, MA, USA) and treated with DNase I (Invitrogen, Carlsband, CA, USA). cDNA synthesis was performed with High Capacity cDNA Reverse Transcription Kit (Applied Biosystems, Foster City, CA) according to the manufacturer's instructions. qPCR was carried out in a total of 10 µl, containing PowerUp™ SYBR™ Green Master Mix 2x (5 µl) (Applied Biosystems, Foster City, CA), 0,4 µM of each primer, 50 ng of cDNA and nuclease free H₂O. Results were expressed as relative amounts of the target gene using β-actin as inner reference gene, using the cycle threshold (Ct) method. Primers and details are described in **Table 1**.

Alkaline phosphatase (ALP) activity

MC3T3-E1 pre-osteoblastic cells in suspension (75×10^3 cells/mL) were seeded in 6-wells dish plate (polystyrene group) or Ti-discs (test's groups) until 85–90% of confluence. Thereafter, the cells were stimulated to differentiate by remaining then under differentiation

medium containing ascorbic acid (50 µg/mL) and β-glycerophosphate (10 mM) during 10 days. Thereafter, the adherent cells were rinsed with ice-cold PBS and incubated for 30 minutes at room temperature with ALP assay buffer (100 mM of Tris-HCl, pH 9.0, 1 mM of MgCl₂) containing 1% Triton X-100. The cell extracts were removed from dishes, centrifuged, and used for the enzyme assay. The ALP activity was determined using 5 mM of pNPP as substrate. One unit of enzyme activity was defined as the amount of enzyme that converted 1 µmol of substrate to product per minute. Protein concentrations were determined by the Lowry method.

Statistical analysis

Mean values and standard deviation obtained for each test were calculated, and one-way ANOVA was performed (alpha error type set to 0.05) when adequate, with Bonferroni corrected post-test, or non-parametric analysis, using GraphPad Prism 5 (GraphPad Software, USA).

RESULTS

Firstly, the surfaces were subjected to methodologies for evaluating surface properties. Atomic force micrographs showed that there is a significant difference among the titanium-texturized surfaces evaluated in this study. The nano-scaled topography promoted by blasting HA on the surfaces was confirmed by AFM (**Fig.1**). In addition, the topography modifications influenced the total surface energy and they were decisive to wettability, significantly impacting water contact angle (**Table 2**).

Pre-osteoblast morphological changes are dependent on titanium surface texturing.

Pre-osteoblast cells were seeded on Mac and nHA Ti-discs and immediately after 4 hours, the Ti discs were subjected to Scanning Electron Microscopy (SEM) in order to evaluate pre-osteoblast morphological changes. Comparing the morphological changes, it is clear that nHA promoted a better environment to trigger cell spreading while at the same time pre-osteoblast cultured on machined Ti-surface preserved the round up cells morphology (**Fig.2**). Thereafter, these findings were validated by EDX analysis, where we can check the distribution of Carbon (**Fig. 3b, e**) and Titanium (**Fig. 3c, f**) over the electron-micrographs. Note that the peak of carbon is coincident with the cell localization on the micrograph (**Fig. 3b, e**).

Osteoblast adhesion signalling is finely modulated by nHA-modified surface.

Firstly, we evaluated the ability of the surfaces to promote osteoblast adhesion by performing violet crystal assay. Our result showed that DAE and nHA promoted significant increase of

osteoblast adhesion when compared with their immediate control (Mac) (**Fig. 4a**). As adsorbed protein as a coating in the Ti discs surfaces could affect cell adhesion, we investigated protein concentration forming a thin film on the Ti Surfaces. In fact, **Fig. 4b** shows that protein concentration profile on Ti-surfaces was variable, suggesting that nHA seems to adsorb more protein from serum.

This result prompted us to analyse signaling protein involved with cell adhesion. In this sense, we have evaluated the phosphorylation of both FAK (Y397) and Src (Y416). Both proteins were increased in response to DAE and nHA (**Fig. 5**), corroborant with the profile of cell adhesion (**Fig. 4a**). The **Fig.5a** presents representative blots obtained in this work, while **Figs.5b-c** shows a densitometry analysis.

Nano HA-blasted titanium surface promotes anti-apoptotic signalling.

In order to understand the osteoblast performance on titanium surfaces, we also studied cell viability. Our result shows that both DAE and nHA did not interfere on osteoblast viability when compared to the immediate control group, the machined surface (**Fig. 6a**). Thereafter, we investigated if titanium surfaces triggered cell death signalling by evaluating the Bax/Bcl2 ratio. Our results showed that Bax and Bcl2 expressions (**Fig. 6b**) were thinly modulated when osteoblast were cultured on titanium surfaces; however, the Bax/Bcl2 ratio decreased (**Fig. 6e**) in those evaluated groups, mainly in response to nHA surfaces. All western-blotting panels showed in this work were normalized with β -actin expression, here considered as a housekeeping control (**Figs. 6c,d**).

Titanium-texturing surfaces promote osteoblast survival/proliferation signalling.

Later, pre-osteoblasts were cultured on the different titanium-modified surfaces for 4 hours and the biological samples collected to evaluate cell signalling responsible to cell survival and proliferation and in this sense we have checked Ras-Raf-Mek-p42/44 mapk signalling. Our results showed that Ras-Raf-Mek- p42/44 mapk signalling was involved (**Fig. 7a**) in response to titanium surfaces, involving the phosphorylation of MEK. It is important to mention that texture modified DAE and nHA promoted a significant increase of Raf (**Fig. 7c**), suggesting this protein involvement with other signalling pathway. Also, all western-blotting panels showed in this work were normalized with β -actin expression, here considered as a housekeeping control (**Figs. 7b-e**).

Titanium-texturing surfaces promote late osteoblast differentiation.

The osteoblast differentiation was evaluated by investigating osteogenic signal transducers as RUNX2 and OSTERIX, Osteocalcin by qPCR and ALP activity by biochemical dosages, as described in Zambuzzi et al. (2014). For this purpose, we decided to evaluate both direct and indirect effect of the Ti modified surfaces on the osteoblast differentiation, where in the indirect manner the cells were treated with the conditioned medium from the titanium samples (**Fig.8a**) while in the direct manner the cells were grown directly on the top of discs (**Fig.8e**). Both osteogenic transcription factors, RUNX2 (**Fig.8b,f**) and OSTERIX (**Fig.8c,g**), were up-modulated by the DAE and nHA, independently of the manner, direct or indirectly. However, the nHA stimulated even more RUNX2 transcripts at the direct interaction (**Fig.8f**). Osteocalcin was not significantly modulated (**Fig.8d,h**), maybe because it is a late osteoblast differentiation biomarker and we subjected the osteoblast to the discs up to 10 days. Finally, our results showed that all of the 3 texturized Ti surfaces stimulated ALP activity in osteoblast cultured on them for 10 days (**Fig. 8**); with nHA provoking a significant increase, when considered $p < 0.05$ (*).

Altogether, our results showed that different titanium surface texturing promoted crucial intracellular signalling pathways, mainly responsible for cell adhesion and proliferation. In this sense, **Fig. 9** summarizes the mainly signalling network involved with cell adaptation and performance on titanium surfaces evaluated in this study and we suggest that those proteins are biomarkers of this event.

DISCUSSION

Biotechnology approaches for modification of implant surfaces have been identified as an important strategy to reduce the rehabilitation time of patients suffering edentulism (Dang et al., 2016; Sohrabi et al., 2012). In this sense, the development of novel bio-functionalizing surfaces on titanium alloys has been proved to be fundamental for enhancing osteoprogenitor cells performance and thus accelerating bone neo-formation surrounding implanted devices, positively impacting implant osteointegration (Kulkarni et al., 2015; Longo et al., 2016). In this sense, our group has been devoted to investigate the cell signalling mechanisms involved in the response to different biomaterials (Gemini-Piperni et al., 2014a; Gemini-Piperni et al., 2014b; Zambuzzi et al., 2014) in order to mine intracellular biomarkers related to this scenario. In this context, we have proposed the importance of Src and FAK involvement as signalling proteins identifying texturing of substrate surfaces (Zambuzzi et al., 2009; Zambuzzi et al., 2010). We have also discussed in this regard that cellular attachment is a very important early biological event responsible for integrating implanted devices to whole bone. In addition, we have also considered the protein coating on implants previous to cell

Accepted Preprint

attachment. To address this issue, we have shown that different texturized titanium surfaces provide differential protein adsorption, mainly related to surface roughness (Zambuzzi et al., 2014). Our results are in agreement with our previously published data, when nano-HA-blasted titanium surface adsorbs a higher concentration of serum proteins than others. Generally speaking, however, this coating of proteins on implantable surface promotes a bio-functionalizing environment able to guide cell adaptation at early interaction by activating intracellular mechanisms to induce either acceptance or rejection of the implant by determining which and how many cells will populate the surface (Barkarmo et al., 2014a; Kulkarni et al., 2015).

Physicochemical properties of the surface, such as wettability (evaluated by water contact angle) and surface topography (evaluated by Atomic Force Microscopy), interferes profoundly cell adhesion, spreading, proliferation and late differentiation. Owing to a hierarchical sequence of biological surroundings to implantable devices, water contact initiates a complex time-line favouring or not the tissue repair. Surface wettability drives the adsorption of proteins, establishing a biological coating and impacting late cell interaction. Our results showed that there is a significant difference on the topography of the titanium surfaces evaluated in this study and it reflected on the wettability. **It is usually reported that cell adhesion requires a moderate hydrophilicity but cell performance is negatively modulated when the material becomes very hydrophilic.**

To note, during eukaryotic cell adhesion, both FAK and Src proteins are responsible for modulating intracellular mechanisms to control cell interaction/matrix upon integrin activation (Barkarmo et al., 2014b; Zambuzzi et al., 2014). We have recently shown that intracellular mechanisms via activation of integrin/FAK/Src pathway promote the rearrangement of cytoskeleton rearrangement and it seems decisive for cell adapting on different surface roughness by determining cell morphology. In this work, we showed that pre-osteoblasts cultured on different texturized Ti surfaces promoted profound morphological changes, here analysed by SEM. Briefly, our electron micrographs showed that pre-osteoblasts cultured on nHA present a more immediate spreading than when on machined surfaces (control surface). This finding is in agreement with Gaviria et al. (2014) that proposed that roughed surfaces produce cells orientation and guide their locomotion affecting cell shape and function (Gaviria et al., 2014). In addition, we also validated these results with EDX approach by co-localizing carbon and titanium. Importantly, the observed morphological changes were accompanied by the activations of both FAK and Src, analysed here by phosphorylation sites of both signalling proteins. Thus, we believe that these morphological changes during cell adaptation are a FAK and Src-dependent manner, as already reported previously for osteoblasts adhesion on polystyrene surfaces (Zambuzzi et al.,

2009). At this point, we believe that FAK and Src recognize physicochemical properties of the surfaces and they are considered as interesting biomarkers of cell-surface interactions. Later, we have shown that critical to cell survival (Ras/Raf /MEK/Erk) was required in pre-osteoblasts cultured on Ti texturized surfaces for 4 hours of adhesion, mainly in osteoblasts cultured on nHA surfaces. Another important point to discuss was the influence of nHA on promoting osteoblast differentiation by significantly up-regulating classical biomarkers as RUNX2 and Alkaline phosphatase activity when pre-osteoblast were grown directly on titanium discs. These characteristics influence the biological response to implantable devices by accelerating tissue healing and later osseointegration (Dang et al., 2016; Longo et al., 2016). Regarding biofunctionalizing nHA surface, the intimate mixture of the coating components allows lower processing temperatures preventing undesired phase transitions and a high homogeneity of the film is expected (Gottlander et al., 1997; Meirelles et al., 2008).

Altogether our results showed for the first time that nano-hydroxyapatite-blasted titanium surface clearly promotes an ideal environment for pre-osteoblast performance by activating crucial signalling network. In general, we have stated that understanding intracellular signalling involved on the mechanisms of osteoblast adhesion, proliferation, and differentiation on implantable devices is fundamental for the successful design of novel bioengineered materials, potentially decreasing the repair time, thereby allowing faster patient rehabilitation.

ACKNOWLEDGEMENTS

We would like to thank FAPESP (Proc. Nrs. 2014/22689-3, 2015/03639-8) and CNPq (Proc. Nr. 301966/2015-0) for the financial support and Prof. Margarida Juri Saeki for the S.E.M. images acquirement. Also, we would like to thank to Electron Microscopy Center, IBB, UNESP, Botucatu – SP, Brazil.

COMPETING FINANCIAL INTERESTS

The authors declare no competing financial interests.

REFERENCES

- Asati V, Mahapatra DK, Bharti SK. 2016. PI3K/Akt/mTOR and Ras/Raf/MEK/ERK signaling pathways inhibitors as anticancer agents: Structural and pharmacological perspectives. Journal Article. *Eur. J. Med. Chem.* **109**:314–341.
- Barkarmo S, Andersson M, Currie F, Kjellin P, Jimbo R, Johansson CB, Stenport V. 2014a. Enhanced bone healing around nanohydroxyapatite-coated polyetheretherketone implants: An experimental study in rabbit bone. *J. Biomater. Appl.* **29**:737–47.
- Barkarmo S, Andersson M, Currie F, Kjellin P, Jimbo R, Johansson CB, Stenport V. 2014b. Enhanced bone healing around nanohydroxyapatite-coated polyetheretherketone implants: An experimental study in rabbit bone. Journal Article, Research Support, Non-U.S. Gov't. *J. Biomater. Appl.* **29**:737–747.
- Bergeron JJM, Di Guglielmo GM, Dahan S, Dominguez M, Posner BI. 2016. Spatial and Temporal Regulation of Receptor Tyrosine Kinase Activation and Intracellular Signal Transduction. JOURNAL ARTICLE. *Annu. Rev. Biochem.*
- Bertazzo S, Zambuzzi WF, Campos DDP, Ferreira C V, Bertran CA. 2010a. A simple method for enhancing cell adhesion to hydroxyapatite surface. Journal Article, Research Support, Non-U.S. Gov't. *Clin. Oral Implants Res.* **21**:1411–1413.
- Bertazzo S, Zambuzzi WF, Campos DDP, Ogeda TL, Ferreira C V, Bertran CA. 2010b. Hydroxyapatite surface solubility and effect on cell adhesion. *Colloids Surfaces B Biointerfaces* **78**:177–184.
<http://www.sciencedirect.com/science/article/pii/S0927776510001153>.
- Cavagis A, Takamori E, Granjeiro J, Oliveira R, Ferreira C, Peppelenbosch M, Zambuzzi W. 2014. TNFalpha contributes for attenuating both Y397FAK and Y416Src phosphorylations in osteoblasts. Journal Article, Research Support, Non-U.S. Gov't. *Oral Dis.* **20**:780–786.
- Dang Y, Zhang L, Song W, Chang B, Han T, Zhang Y, Zhao L. 2016. In vivo osseointegration of Ti implants with a strontium-containing nanotubular coating. Journal Article. *Int. J. Nanomedicine* **11**:1003–1011.
- Di Liddo R, Paganin P, Lora S, Dalzoppo D, Giraudo C, Miotto D, Tasso A, Barbon S, Artico M, Bianchi E, Parnigotto PP, Conconi MT, Grandi C. 2014. Poly-epsilon-caprolactone composite scaffolds for bone repair. Journal Article. *Int. J. Mol. Med.* **34**:1537–1546.
- Fernandes GVO, Cavagis ADM, Ferreira C V, Olej B, Leao M de S, Yano CL, Peppelenbosch M, Granjeiro JM, Zambuzzi WF. 2014. Osteoblast adhesion dynamics: a possible role for ROS and LMW-PTP. Journal Article, Research Support, Non-U.S. Gov't. *J. Cell. Biochem.* **115**:1063–1069.
- Gaviria L, Salcido JP, Guda T, Ong JL. 2014. Current trends in dental implants. Journal Article, Review. *J. Korean Assoc. Oral Maxillofac. Surg.* **40**:50–60.

- Gemini-Piperni S, Milani R, Bertazzo S, Peppelenbosch M, Takamori ER, Granjeiro JM, Ferreira C V, Teti A, Zambuzzi W. 2014a. Kinome profiling of osteoblasts on hydroxyapatite opens new avenues on biomaterial cell signaling. Journal Article, Research Support, Non-U.S. Gov't. *Biotechnol. Bioeng.* **111**:1900–1905.
- Gemini-Piperni S, Takamori ER, Sartoretto SC, Paiva KBS, Granjeiro JM, de Oliveira RC, Zambuzzi WF. 2014b. Cellular behavior as a dynamic field for exploring bone bioengineering: a closer look at cell-biomaterial interface. Journal Article, Research Support, Non-U.S. Gov't, Review. *Arch. Biochem. Biophys.* **561**:88–98.
- Gottlander M, Johansson CB, Wennerberg A, Albrektsson T, Radin S, Ducheyne P. 1997. Bone tissue reactions to an electrophoretically applied calcium phosphate coating. *Biomaterials.* **18**:551–557.
- Henkel J, Woodruff M, Epari D, Steck R, Glatt V, Dickinson I, Choong P, Schuetz M, Huttmacher D. 2013. Bone Regeneration Based on Tissue Engineering Conceptions – A 21st Century Perspective. *Bone Res.* **1**:216–248.
<http://dx.doi.org/10.4248/BR201303002>.
- Hu N, Feng C, Jiang Y, Miao Q, Liu H. 2015. Regulative Effect of Mir-205 on Osteogenic Differentiation of Bone Mesenchymal Stem Cells (BMSCs): Possible Role of SATB2/Runx2 and ERK/MAPK Pathway. Journal Article, Research Support, Non-U.S. Gov't. *Int. J. Mol. Sci.* **16**:10491–10506.
- Jiang T, Guo L, Ni S, Zhao Y. 2015. Upregulation of cell proliferation via Shc and ERK1/2 MAPK signaling in SaOS-2 osteoblasts grown on magnesium alloy surface coating with tricalcium phosphate. Journal Article, Research Support, Non-U.S. Gov't. *J. Mater. Sci. Mater. Med.* **26**:158.
- Jimbo R, Coelho PG, Bryington M, Baldassarri M, Tovar N, Currie F, Hayashi M, Janal MN, Andersson M, Ono D, Vandeweghe S, Wennerberg A. 2012. Nano hydroxyapatite-coated implants improve bone nanomechanical properties. Comparative Study, Journal Article, Research Support, Non-U.S. Gov't. *J. Dent. Res.* **91**:1172–1177.
- Kulkarni M, Mazare A, Gongadze E, Perutkova S, Kralj-Igli V, Milosevic I, Schmuki P, Igli A, Mozeti M. 2015. Titanium nanostructures for biomedical applications. *Nanotechnology* **26**:62002 (1-18).
- Kjellin P, Andersson M. 2006. SE-0401524-4, assignee. Synthetic nano-sized crystalline calcium phosphate and method of production patent SE527610.
- Longo G, Ioannidu CA, Scotto d'Abusco A, Superti F, Misiano C, Zanoni R, Politi L, Mazzola L, Iosi F, Mura F, Scandurra R. 2016. Improving Osteoblast Response In Vitro by a Nanostructured Thin Film with Titanium Carbide and Titanium Oxides Clustered around Graphitic Carbon. Journal Article. *PLoS One* **11**:e0152566.
- Meirelles L, Arvidsson A, Andersson M, Kjellin P, Albrektsson T, Wennerberg A. 2008.

Nano hydroxyapatite structures influence early bone formation. *J. Biomed. Mater. Res. A.* **87**:299-307.

Salou L, Hoornaert A, Stanovici J, Briand S, Louarn G, Layrolle P. 2015. Comparative bone tissue integration of nanostructured and microroughened dental implants. Journal Article, Research Support, Non-U.S. Gov't. *Nanomedicine (Lond)*. **10**:741–751.

Sohrabi K, Mushantat A, Esfandiari S, Feine J. 2012. How successful are small-diameter implants ? A literature review.

Zambuzzi WF, Fernandes GVO, Iano FG, Fernandes M da S, Granjeiro JM, Oliveira RC. 2012. Exploring anorganic bovine bone granules as osteoblast carriers for bone bioengineering: A study in rat critical-size calvarial defects. *Braz. Dent. J.* **23**:315–321.

Zambuzzi WF, Milani R, Teti A. 2010. Expanding the role of Src and protein-tyrosine phosphatases balance in modulating osteoblast metabolism: Lessons from mice. *Biochimie* **92**:327–332. <http://dx.doi.org/10.1016/j.biochi.2010.01.002>.

Zambuzzi WF, Bonfante EA, Jimbo R, Hayashi M, Andersson M, Alves G, Takamori ER, Beltrao PJ, Coelho PG, Granjeiro JM. 2014. Nanometer scale titanium surface texturing are detected by signaling pathways involving transient FAK and Src activations. Journal Article, Research Support, Non-U.S. Gov't. *PLoS One* **9**:e95662.

Zambuzzi WF, Coelho PG, Alves GG, Granjeiro JM. 2011a. Intracellular signal transduction as a factor in the development of “smart” biomaterials for bone tissue engineering. Journal Article, Review. *Biotechnol. Bioeng.* **108**:1246–1250.

Zambuzzi WF, Ferreira C V, Granjeiro JM, Aoyama H. 2011b. Biological behavior of pre-osteoblasts on natural hydroxyapatite: a study of signaling molecules from attachment to differentiation. Journal Article, Research Support, Non-U.S. Gov't. *J. Biomed. Mater. Res. A* **97**:193–200.

Zambuzzi WF, Bruni-Cardoso A, Granjeiro JM, Peppelenbosch MP, De Carvalho HF, Aoyama H, Ferreira CV. 2009. On the road to understanding of the osteoblast adhesion: Cytoskeleton organization is rearranged by distinct signaling pathways. *J. Cell. Biochem.* **108**:134–144.

FIGURE CAPTIONS

Fig.1. Atomic force micrographs reveal the topography of Ti-texturing surfaces. AFM analysis infer on topography height and three dimensional perspective image showing a $3 \times 3 \mu\text{m}^2$ field representative from Ti-texturing surfaces: Mac (**a**); DAE (**c**); nHA (**e**). Lateral profiles taken from the pre-selected line are displayed on images (**b,d,f**). From these images it is possible to infer a sample roughness ranging from units to hundreds of nanometers. It is possible to verify a fine (nanometric) roughness covering the surface of nHA and going along with the micrometric roughness promoted by the acid etching treatment.

Fig.2. Scanning Electron Microscopy reveals pre-osteoblast morphological changes dependent on titanium-texturing surfaces. Pre-osteoblast cells were seeded in 2 different titanium-texturing surfaces: control (Machined) and nano HA-blasted titanium surfaces up to 4h. Different magnifications (500x and 2000x) were used to obtain SEM images of each group. It is clear to observe that pre-osteoblast cells interacting with nHA surfaces presented a more advanced spreading process when compared to those cultured on machined surfaces (control).

Fig.3. SEM-associated EDX approach validates cell behaviour on different Ti modified surfaces. EDX analyses were performed with 20 kV to detect x-ray characteristic of carbon and titanium containing onto the samples. It can be observed carbon elements identification was coincident with the adherent cells, while titanium elements was also identified on whole sample. Importantly, nano hydroxyapatite-blasted titanium surfaces (nHA) presented a more dispersed carbon distribution coincident with more spreading cells. The differences in the carbon distribution on both evaluated surfaces emphasize the difference in early cell behaviour on each surface.

Fig.4. Cell adhesion on Ti-texturing surfaces is mediated by early protein adsorption from medium. **a.** Firstly, pre-osteoblast cells were treated with conditioned medium from the different Ti-texturing surfaces (conditioned medium was prepared as recommended by ISO 10993-12). After 24h of treating, the pre-osteoblasts were trypsinized and counted by using a haematological chamber. The same amount of cells was seeded and 4h later, the adherent cells were stained with Violet Crystal as mentioned in M&M in details. The results show that pre-osteoblast has a more influence of nHA on cell adhesion performance (* $p < 0.0021$, $n = 12$); **b.** Ti-texturing discs was maintained emerged on cell culture containing FBS 10% up to 24 hours. Thereafter, the adsorbed protein on titanium discs was gently 3x rinsed in 1mL PBS and thereafter the adsorbed protein was mechanically scraped in 500 μL of PBS. These samples were used to measure the amount of protein by using Lowry method at absorbance 570 nm ($n = 6$). Briefly, the results showed there is an influence of Ti-texturing surfaces on protein coating, however it did not express significance among the groups here evaluated. **Note:** Machined (Mac; control); 2. Dual Acid-Etched (DAE), and Dual Acid-Etched nano HA-blasted (nHA).

Fig.5. Both FAK and Src phosphorylations are differentially required in response to nano hydroxyapatite-blasted surface. **a.** To assess signalling proteins involved in early osteoblast response to titanium, we checked the phosphorylation profile of proteins related to focal adhesion components [**b:** Src (Y416) and **c:** FAK (Y925, Y397)]; pre-osteoblasts cells were seeded on Ti-texturing surfaces and after 4h the samples were collected to perform

immunoblotting approach. Both FAK and Src have been activated by all Ti-texturing surfaces evaluated in this study, it was clear that nHA provoked a bigger phosphorylation of both FAK and Src when compared with others. Also, all western-blotting panels showed in this work were normalized with β -actin expression, here considered as a housekeeping control. Note: Machined (Mac; control); 2. Dual Acid-Etched (DEA), and acid-etched nano-HA-blasted (nHA). **Note:** significances were considered when $*p<0.001$, $n=3$.

Fig.6. Ti-texturing surfaces decrease pre-osteoblasts anti-apoptotic signalling. a.

Cytotoxic effects of Ti-texturing surfaces were measured by mitochondrial dehydrogenase activity (MTT assay) represented as a percentage of control (tissue plastic) cell viability. * means statistically significant differences between groups ($*p<0.05$; $n=12$). In order to validate this result, pre-osteoblasts were cultured on different Ti-modified surfaces during 24 hours and thereafter the cell lysate was collected to evaluate Bax and Bcl2 expressions (b), when β -actin expression was used as housekeeping control (b). Letters “c” and “d” bring a densitometries of the bands of Bax and Bcl2, respectively ($n=3$). In addition, Bax/Bcl2 ratio was determined in order to estimate anti- or pro-apoptotic signalling. The letter e shows that Ti-modified surfaces promote anti-apoptotic signalling ($*p<0.0194$), when we stated that Bax/Bcl2 ratio was decreased in comparison to Mac. **Note:** Machined (Mac; control); 2. Dual Acid-Etched (DEA), and acid-etched nano-HA-blasted (nHA).

Fig.7. Ti-texturing surfaces promote osteoblast Ras-Erk signalling. Pre-osteoblasts were cultured on the different Ti-texturing surfaces and after 24 hours they were lysed in order to estimate Ras-Erk axis signalling by performing western-blotting approach. a. Representative blots of Ras, Raf, pMEK (Ser221) e pP42/44-mapk (Thr202/Tyr204). Graphs were built from 3 independent sets of results and obtained from band densitometry (b-e). All bars representing groups was normalized using β -actin expression average. In graphs, * means significant differences ($p<0.05$; $n=3$).

Fig.8. Ti-texturing surfaces promote pre-osteoblast differentiation up to 10 days. “a,e” schematization of the experiment, when pre-osteoblast cells subjected for direct (b-d) or indirect (f-h) responses in order to understand the osteogenic performance in response to the Ti-texturized surfaces (i). After 10 days, the cells were scraped allowing osteogenic transcripts (RUNX2, OSTERIX and OSTEOCALCIN) and Alkaline Phosphatase (ALP) as it was measured by Zambuzzi et al. (2014). Briefly, we have shown that all Ti-texturing surfaces evaluated promoted ALP activity, mainly pronounced by nHA surfaces. To note: *,# mean significances between the groups.

Fig.9. Schematization of signalling proteins proposed in this work. Upon integrin activation there is a recruitment of Focal Adhesion Kinase (FAK), a cytoplasmic protein-tyrosine kinase, and creating a phosphotyrosine docking site for members of the Src family of cytoplasmic tyrosine kinases. We suggest these signalling proteins as biomolecules able to promote cytoskeleton rearrangement necessary during osteoblast adaptation on substrate. Thereafter, Ras-Raf-MEK-ERK cascade couples signals from cell surface receptors to transcription factors, which regulate prevention of apoptosis and induction of cell cycle progression. Altogether, these molecules seem to being responsible to govern osteoblast adaptation on titanium-texturing surfaces.

Figure 1

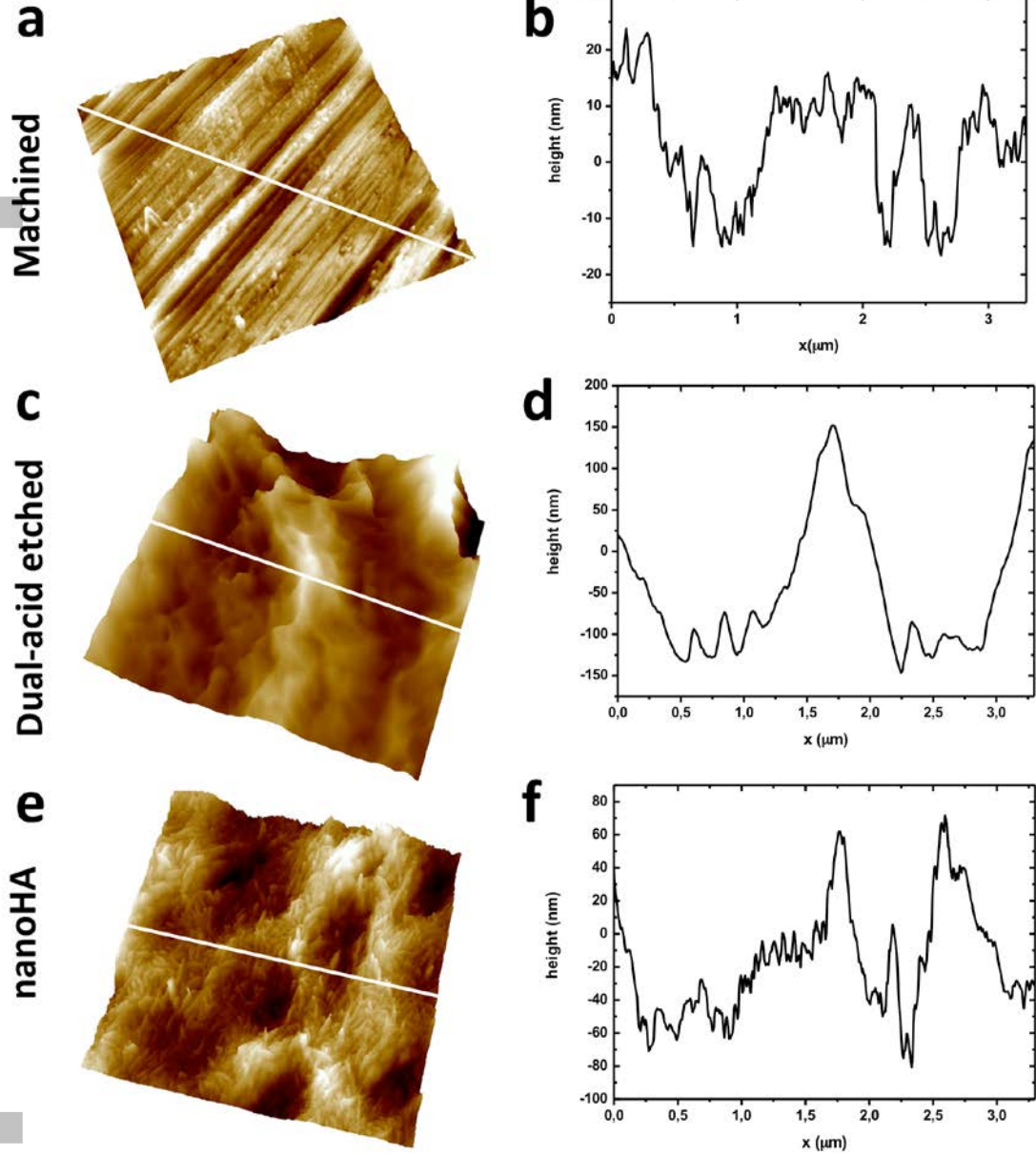


Figure 2

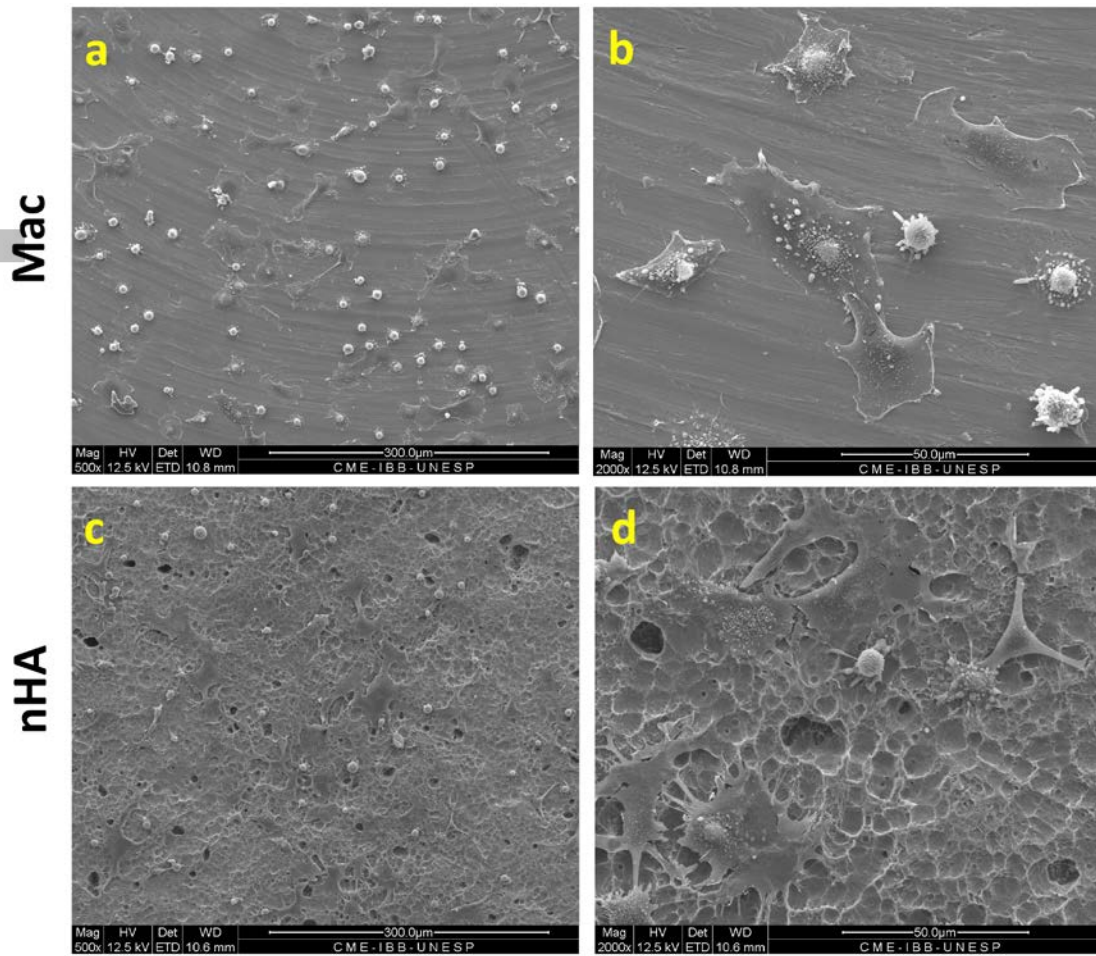


Figure 3

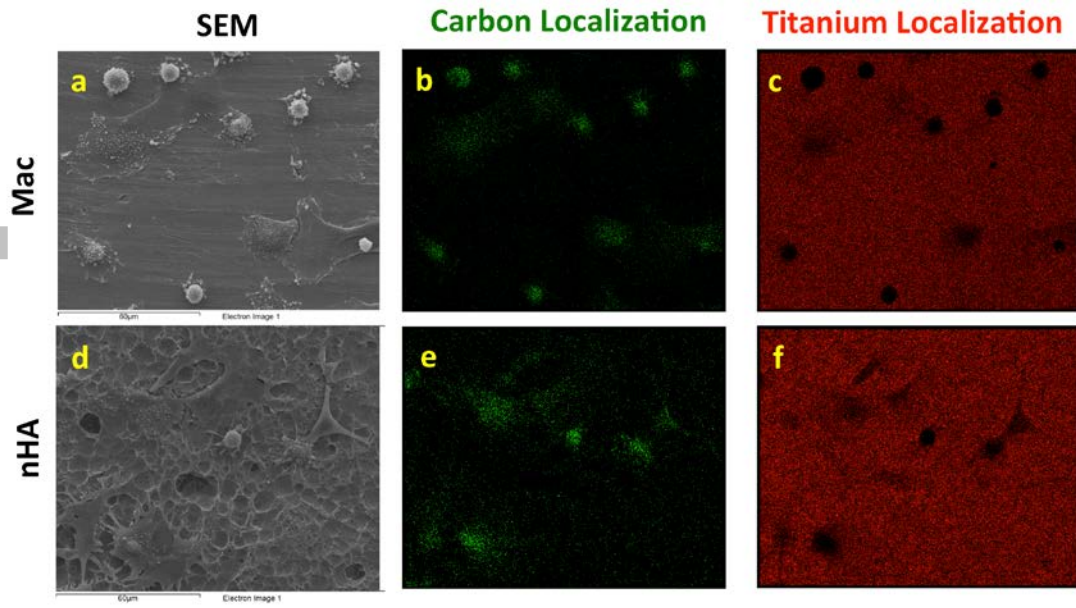


Figure 4

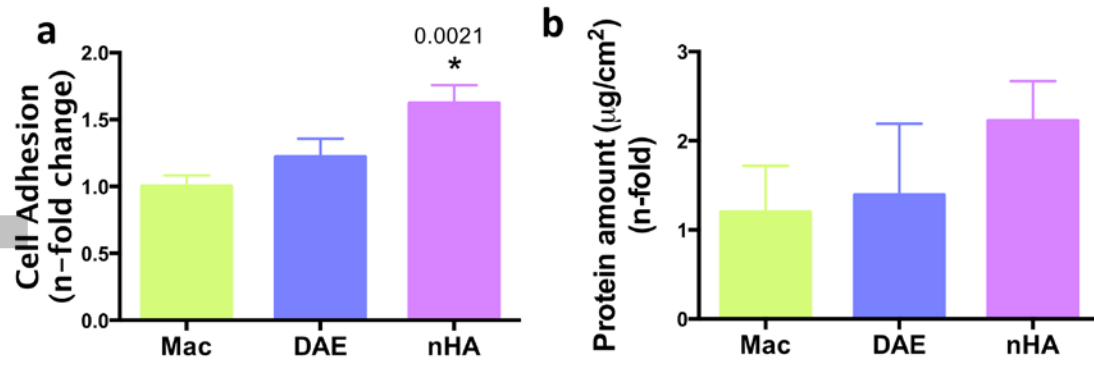


Figure 5

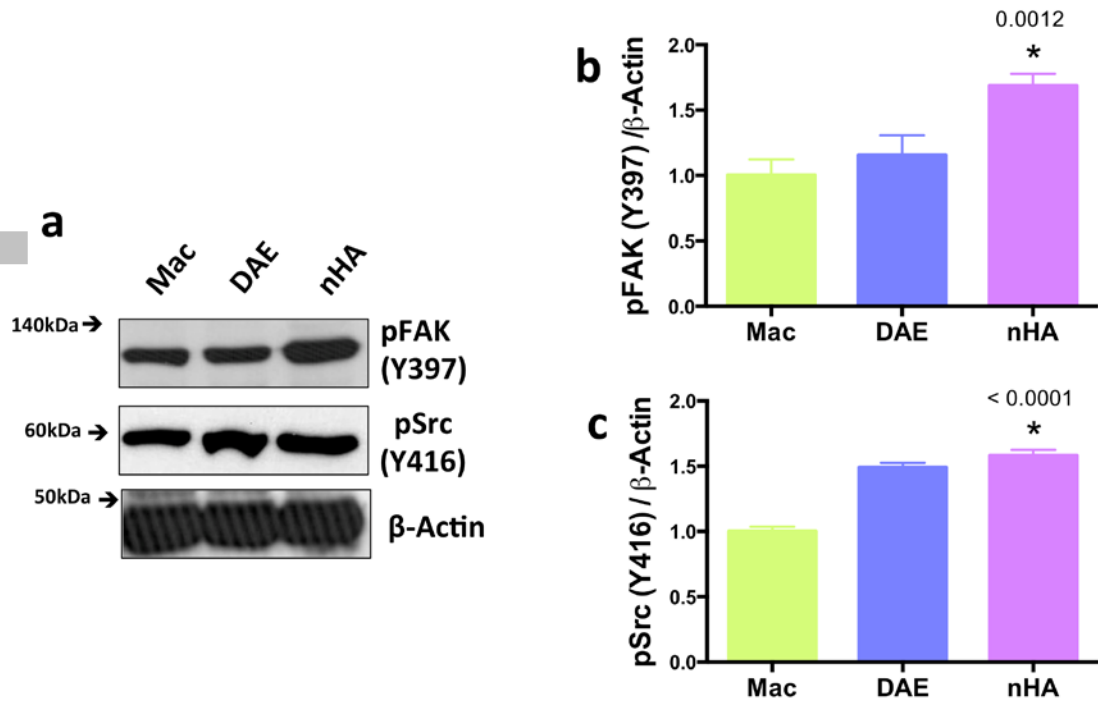


Figure 6

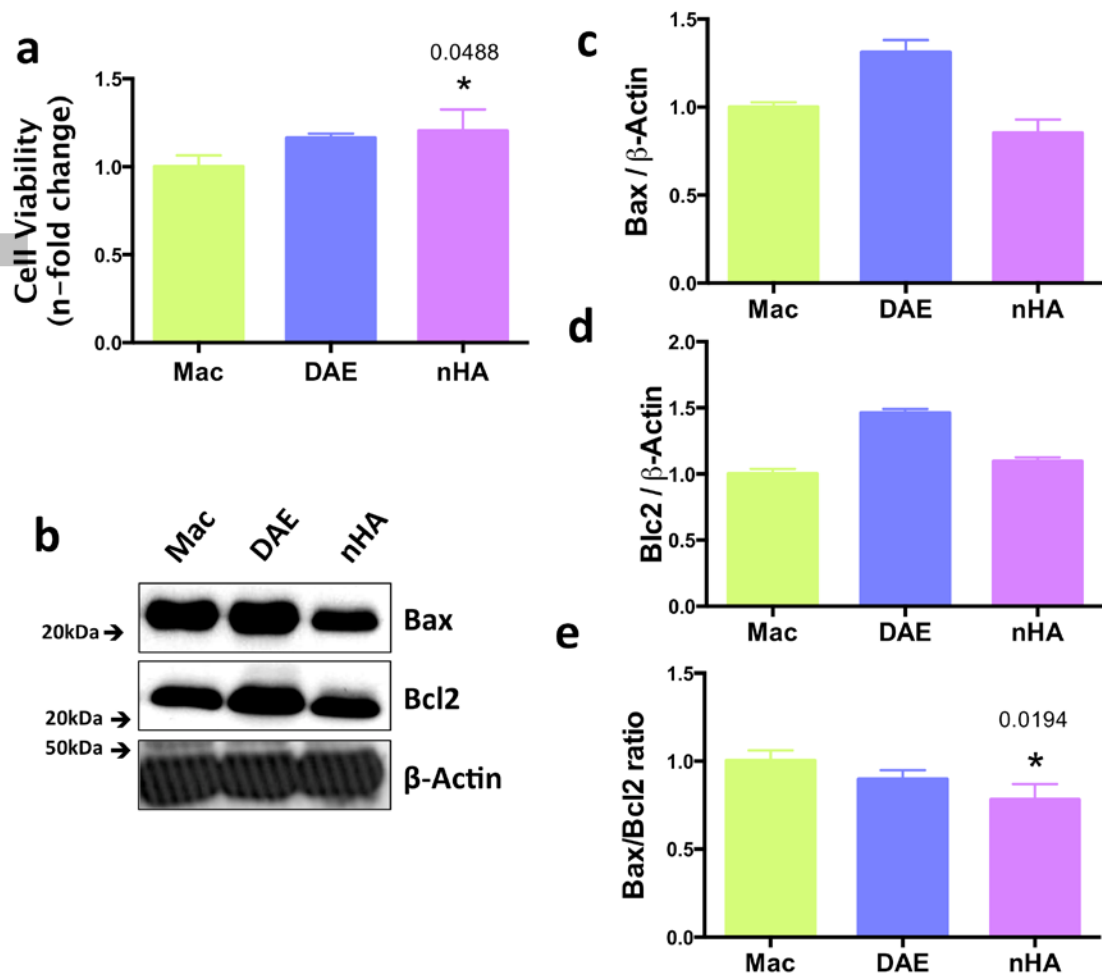


Figure 7

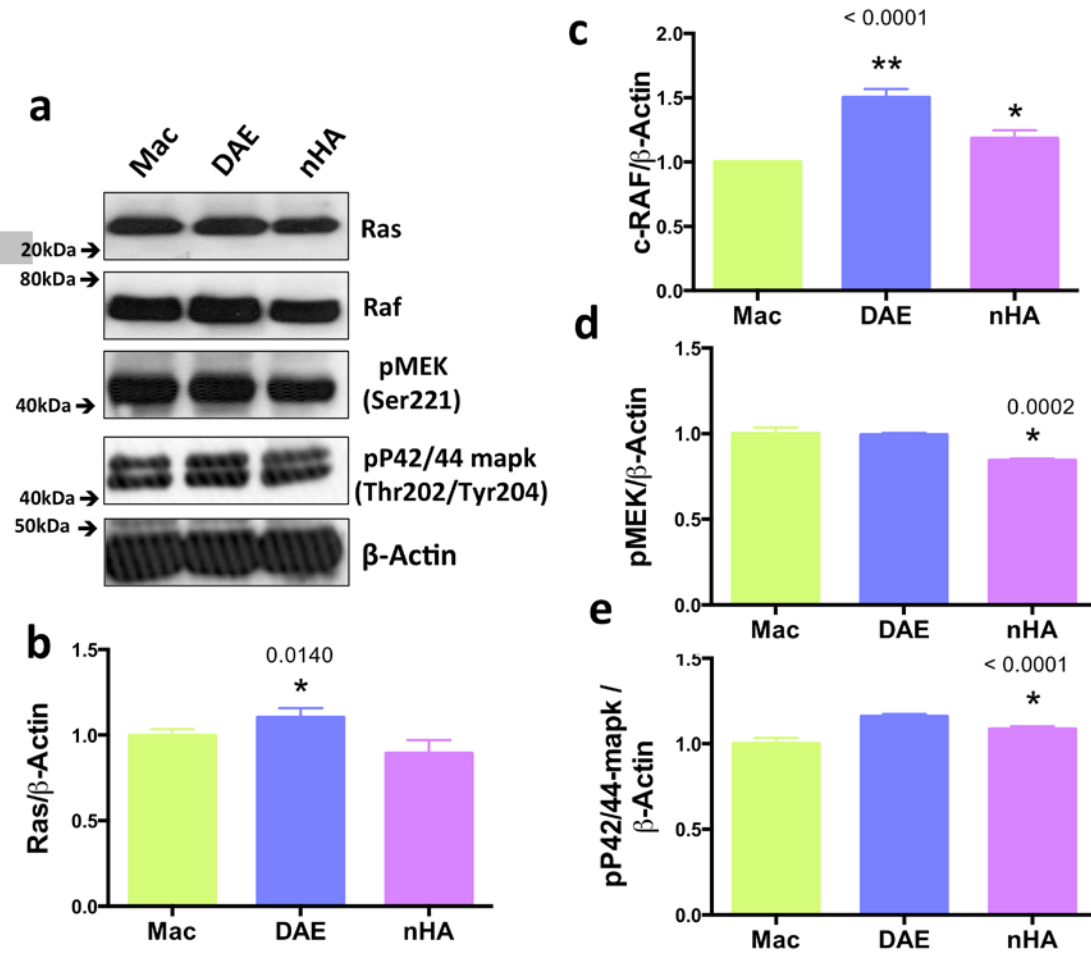


Figure 8

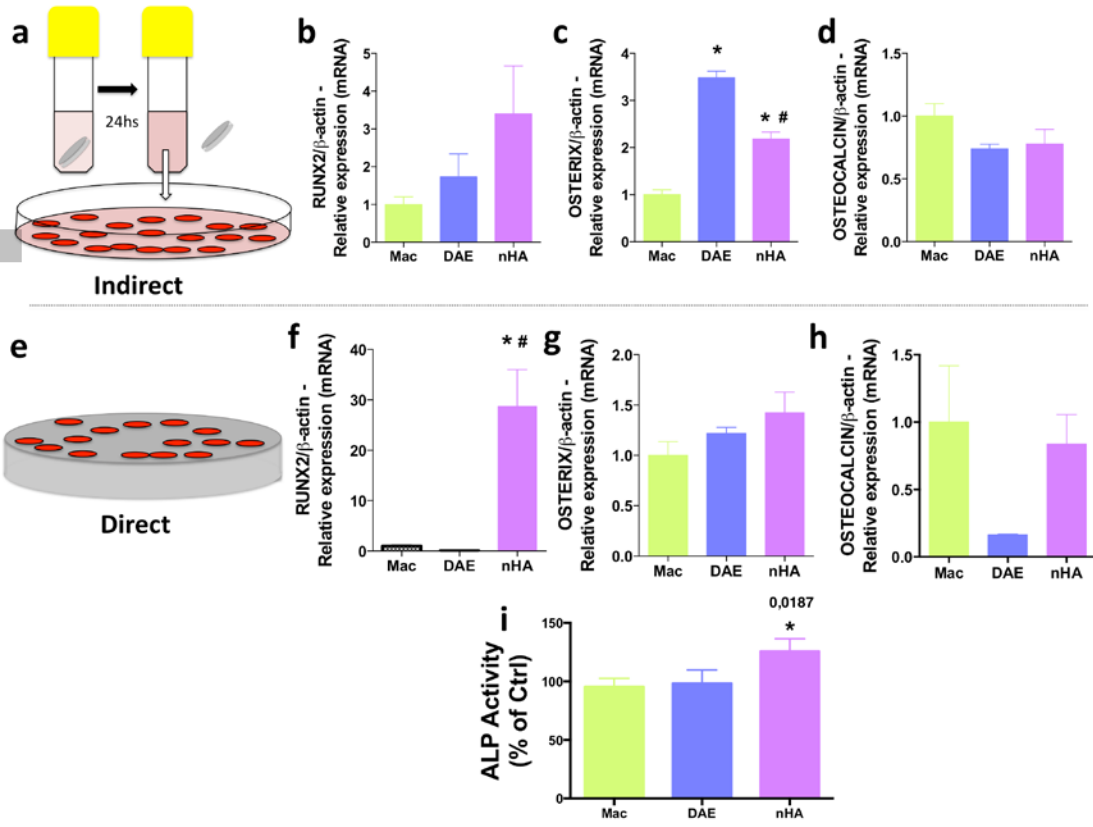


Figure 9

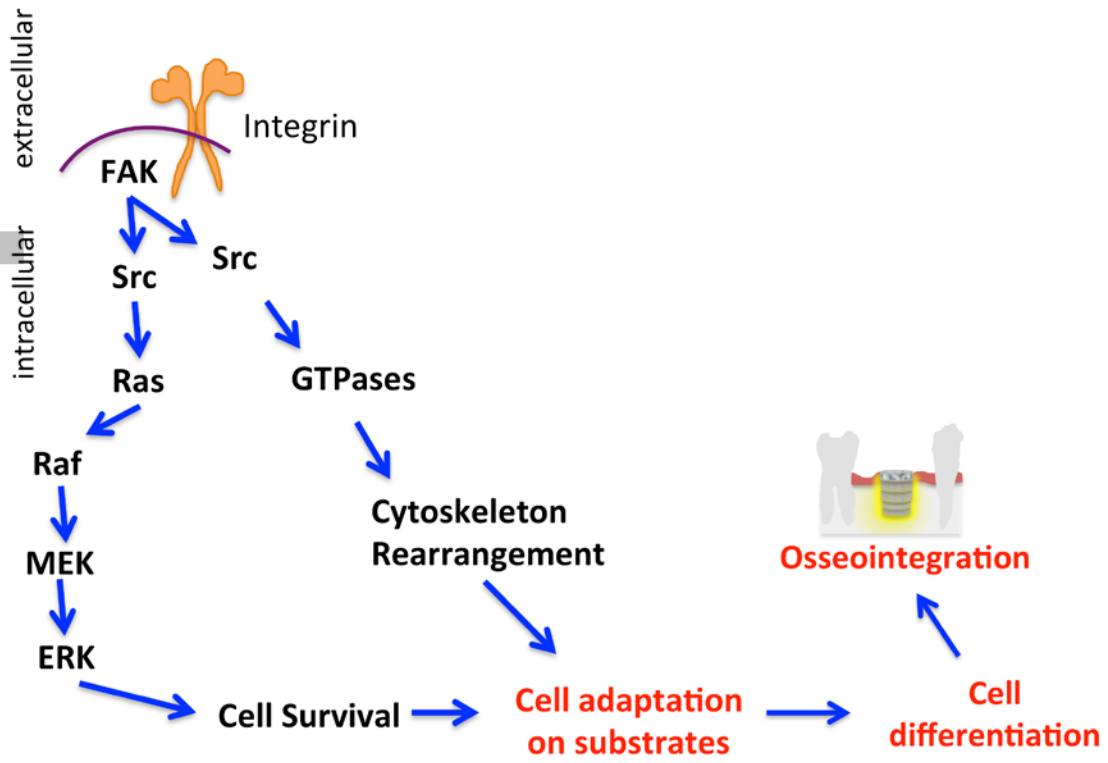


Table 1. Expression primers sequences and PCR cycle conditions.

Gene	Primer	5'-3' Sequence	Reactions Condition
RUNX2	Forward	GGA CGA GGC AAG AGT TTC A	95°C - 3s; 55°C - 8s; 72°C - 20s
	Reverse	TGG TGC AGA GTT CAG GGA G	
Osteocalcin (OCN)	Forward	AGA CTC CGG CGC TAC CTT	95°C - 3s; 55°C - 8s; 72°C - 20s
	Reverse	CTC GTC ACA AGC AGG GTT AAG	
Osterix (OTX)	Forward	CCC TTC CCT CAC TCA TTT CC	95°C - 5s; 56°C - 10s; 72°C - 15s
	Reverse	CAA CCG CCT TGG GCT TAT	
b-actin	Forward	TCT TGG GTA TGG AAT CCT GTG	95°C - 3s; 55°C - 8s; 72°C - 20s
	Reverse	AGG TCT TTA CGG ATG TCA ACG	

Table 2. Wettability and Energy characteristics

	Angle		Total Surface Energy	Polar Component	Dispersive Component
	Water	Diiodomethane			
Mac	81.41 ± 0.01	41.21 ± 0.01	47.53 ± 0.01	7.92 ± 0.00	39.60 ± 0.00
DAE	97.18 ± 0.01	52.84 ± 0.00	36.79 ±	2.78 ±	34.01 ±
nHA	40.95 ± 0.02	39.51 ± 0.01	67.70 ± 0.01	27.32 ± 0.01	40.38 ± 0.00

Mac: Machined; DAE: double-acid etching; nHA: nano hydroxyapatite-blasted surface.